Nonuniform Layer Model of a Millimeter-Wave Phase Shifter

JEROME K. BUTLER, SENIOR MEMBER, IEEE, TRAN-FU WU, AND MARION W. SCOTT, MEMBER, IEEE

Abstract—**The electromagnetic wave propagation of millimeter waves in dielectric waveguides with thin surface plasma layers is characterized. The phase and attenuation of a 94-GHz wave are computed for various surface plasma layer thicknesses as a function of carrier density levels. The electron/hole pairs generated in the vicinity of the dielectric waveguide surface by photo excitation are assumed to have an exponential profile due to either carrier diffusion or the exponential absorption of the optical field. Field computations made for a uniform plasma layer are compared with those of the nonuniform plasma to illustrate the effects of the exponential tails of the carrier profiles on both the phase and attenuation of the millimeter wave. The thin plasma layers slightly affect the field profile of the transverse electric modes (fields polarized parallel to the plasma layer). The transverse magnetic fields are highly distorted at plasma densities greater than 10^{16} cm^{-3}.**

I. Introduction

A FUNDAMENTAL PURPOSE of many electronic devices is to control the amplitude, phase or direction of propagation of electromagnetic waves. This is usually accomplished by passing the electromagnetic wave through a medium whose properties (refractive index and extinction coefficient, or complex dielectric constant) can be dynamically controlled. A variety of methods exist for dynamically controlling the dielectric constant of material, including the application of an electric, magnetic, or acoustic field to the material. These techniques have been applied with considerable success to devices which operate in the microwave and in the optical regions of the spectrum. Attempts to apply these methods to the millimeter-wave spectral region have not been as successful. Reliable, high-performance millimeter-wave components such as dynamically controlled phase shifters, limiters, filters, etc., are not yet available. The development of these components is a necessary step toward fully utilizing the millimeter-wave region of the spectrum.

A technique for controlling the dielectric constant of materials which shows particular promise at millimeter-wave frequencies is the use of free-carrier effects in the material. The well-known Drude–Lorentz theory expresses the dependence of the complex dielectric constant on the density of free carriers [1]. The theory predicts that the plasma effects on the dielectric constant will be pronounced at the lower frequencies (below optical frequencies). This occurs because at frequencies above the free-carrier collision frequency which characterizes carrier relaxation in the material, the functional dependence of the real and imaginary parts of the dielectric constant are related to the inverse second and third powers of the frequency, respectively.

One of the more promising applications of the effect is the creation of millimeter-wave phase shifters. In these devices, the electromagnetic waves are confined to a dielectric waveguide (usually fabricated of silicon or gallium arsenide). A plasma region is then created in the waveguide, perturbing the propagating mode. The presence of the plasma region alters the wave velocity relative to that in the unperturbed waveguide, resulting in a net phase shift at the output.

The use of this technique for the fabrication of a practical device requires a method of dynamically creating the plasma region in the waveguide. Two methods have been reported in the literature. One method requires injection of electrons from contacts [2]–[4]. Experimental measurements of the propagation characteristics of the plasma injection devices show relatively high losses per degree of phase shift [5], [6]. However, this disadvantage has been minimized by an alternate approach using photo generation of carriers [7], [8]. An optical field is used to illuminate specified regions of the waveguide; the photons are absorbed, creating electron/hole pairs, and thus forming the plasma region. Because the plasma region is created in a thin layer near the surface of the waveguide, the losses are minimized and theory predicts a high phase shift per decibel of loss.

The theoretical model used to analyze this structure [7], [8] assumed that the thin plasma region had a uniform free-carrier density of specified thickness. To estimate the wave behavior, Maxwell's equations were solved for the multilayer dielectric waveguide. The resulting field solutions were a first-order approximation and illustrated the basic device performance. However, some subtle characteristics of the plasma/dielectric waveguide cannot be explained using the simple four-layer dielectric waveguide model. Consequently, we have modeled the dielectric/plasma waveguide using a more accurate nonuniform dielectric profile characterizing the plasma created by an exponentially absorbed optical beam. We have solved Maxwell's equations in the nonuniform layer using the multipoint boundary-value routine COLSYS [9], [10]. Both transverse electric (TE) and transverse magnetic (TM) waves have been analyzed. The exponential plasma profile

Manuscript received May 20, 1985; revised July 29, 1985.

J. K. Butler and T. F. Wu are with Southern Methodist University, Dallas, TX 75275.

M. W. Scott is with the LTV Aerospace and Defense Company, Dallas TX 75265-003.

IEEE Log Number 8405820.

0018-9480/86/0100-0147$01.00 ©1986 IEEE

has been explored in detail because it is the form of the plasma density resulting from both the absorption of optical radiation and carrier diffusion.

Some important differences in the results of the two models are illustrated. One major difference is that the decrease in attenuation with increasing plasma density predicted by the uniform density model does not occur in the nonuniform case. The exponential tail of free carriers extending into the waveguide continues to give a loss as the density increases because the fields cannot be completely extinguished from the highly absorbing plasma region. (This is in contrast to the uniform density model, where the fields are pushed from the high-density plasma region.) Loss is plotted as a function of plasma density for the device, allowing a comparison with the other millimeter-wave phase shifters. The fundamental mode in the waveguides is also plotted to show the effects of the plasma layer on the electric field shapes.

II. Uniform-Layer Model

The uniform layer model is useful for estimating the basic performance of the dielectric waveguide and will be reviewed for comparison to the nonuniform structure. Further, we will illustrate calculations that show the shapes of the fields in the dielectric waveguide with a thin plasma region at one surface of the dielectric slab.

In all of our computations, we assume the dielectric structure as shown in Fig. 1 has infinite extent along the y-direction. The calculated complex propagation constants will only be slightly different form those obtained assuming a rectangular waveguide [11]. The plasma region of width ω is assumed to have a uniform density of free carriers. In the absence of carrier injection, the plasma layer is the same semiconductor material as the bulk of the waveguide. Free carriers are injected in this region by photo excitation. The existence of the free carriers, or plasma, changes the dielectric constant of the semiconductor according to the Drude–Lorentz formula

$$\kappa(\omega) = \kappa_\infty \left(1 - \sum_i \frac{\omega_i^2}{\omega^2 + \gamma_i^2} - \frac{j}{\omega} \sum_i \frac{\omega_i^2 \gamma_i}{\omega^2 + \gamma_i^2}\right) \quad (1)$$

where the subscript i denotes the different kinds of carriers and

κ_∞ dielectric constant in the absence of free carriers,
τ_i relaxation time of carrier i,
$\gamma_i = 1/\tau_i$,
$\omega_i = (N_i q^2/m_i \epsilon_0 \kappa_\infty)^{1/2}$ = plasma frequency,
q electronic charge,
ϵ_0 permitivity of free space,
m_i effective mass of carrier i,
N_i number density of charge carrier i.

κ is related to the optical constants by the equation

$$\kappa(\omega) = (n - jk)^2 \quad (2)$$

where n is the refractive index and k is the extinction coefficient. The material parameters for Si and GaAs required in (1) can be obtained from the literature. The dielectric constant of these materials has recently been measured with high accuracy [12]. Other required material properties, such as the mobility μ_i and effective mass m_i are given in several sources (see, for example, [13]). The bulk relaxation time can be computed using

$$\tau_i = \frac{m_i \mu_i}{q}. \quad (3)$$

Silicon has both longitudinal m_l and transverse m_t effective masses for free electrons. The conductivity effective mass m_e is given by [13]

$$\frac{1}{m_e} = \frac{1}{3}\left(\frac{2}{m_t} + \frac{1}{m_l}\right). \quad (4)$$

Silicon also has both light and heavy holes. Each of these contribute to (1) as a separate charge carrier. The properties of Si and GaAs required in the Drude–Lorentz equations are summarized in [8], along with plots of n and k as functions of free-carrier number density.

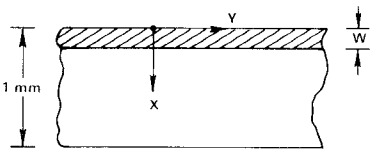

Fig. 1. Dielectric waveguide with surface plasma layer The waveguide thickness is 1 mm and the plasma layer thickness is W .

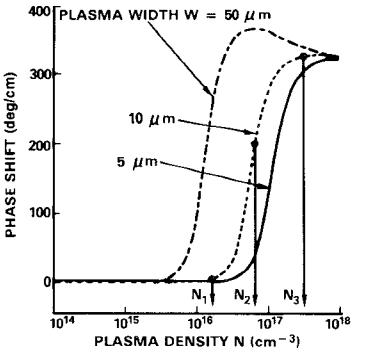

(a)

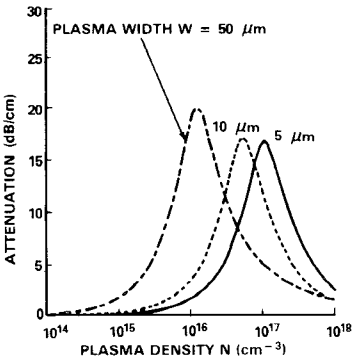

(b)

Fig. 2. The propagation characteristics for a TM mode in a silicon waveguide with uniform plasma layers of various thickness, as a function of carrier density. (a) The phase shift and (b) the attenuation.

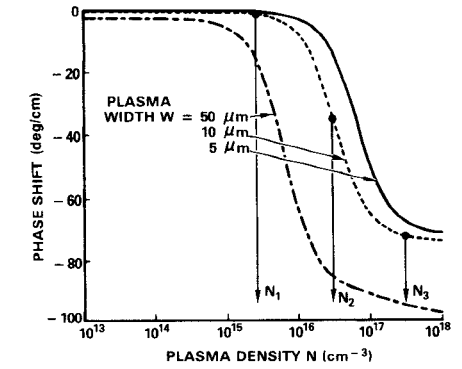

(a)

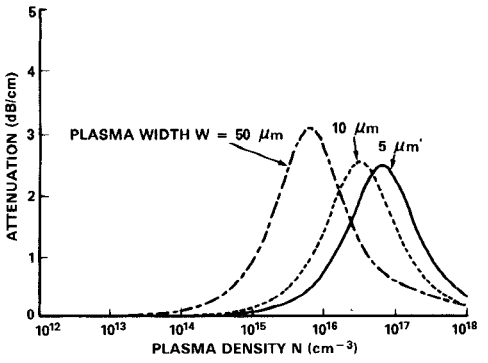

(b)

Fig. 3. The propagation characteristics for a TE mode in a silicon waveguide with uniform plasma layers of various thicknesses, as a function of carrier density. (a) The phase shift and (b) the attenuation.

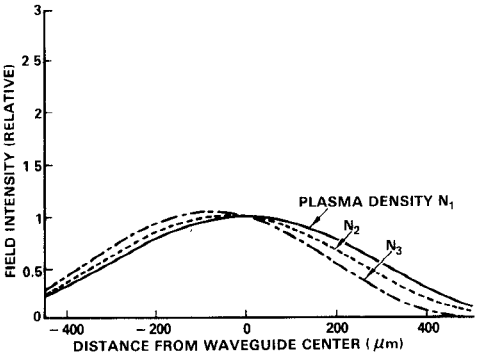

Fig. 4. The electric field intensity for the TE mode for various carrier densities in the silicon waveguide with a uniform plasma layer of 10-μm thickness. The plasma layer extends from 490 to 500 μm.

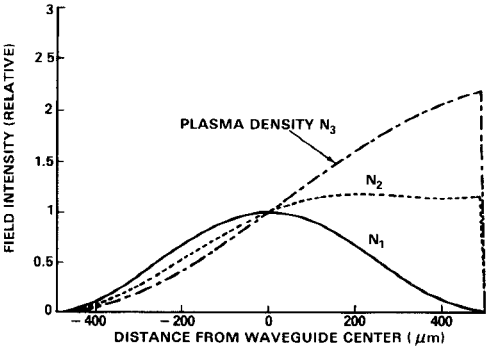

Fig. 5. The electric field intensity for the TM mode for various carrier densities in the silicon waveguide with a uniform plasma layer of 10-μm thickness. The plasma layer extends from 490 to 500 μm.

When this device is used as a phase shifter, the amount of phase shift it produces is calculated from the difference in the propagation constants when the plasma is present from that obtained in its absence. The real part of the propagation constant gives the attenuation when the plasma is present. Plots of the phase shift and attenuation for the TM mode as a function of plasma density are given in Fig. 2 for Si. These plots are in good agreement with the results shown in [7] and [8]. Fig. 2 indicates that very high values of phase shift per unit length can be obtained when the plasma density is sufficiently high. The figure also indicates that attenuation can be reduced, even for the thicker plasma layers, by sufficiently increasing the plasma density.

The plots in Fig. 2 are for the TM mode, which exhibits the highest phase shift. The phase shift and attenuation of the TE mode in Si are shown in Fig. 3. The curves are of the same general shape as for the TM mode, but the magnitude of the phase shift is less.

Some insight into the reasons for the device behavior can be obtained from plots of the field intensity distribution in the waveguide. The fields are shown in Fig. 4 for the TE mode and Fig. 5 for the TM mode. The fields have been plotted for three plasma densities—one just prior to the "threshold" of the phase shift curves, one in the middle of that curve, and one at the plasma of high phase shift attained at the end of the rapid rise. These points are shown in Figs. 2 and 3. Fig. 4 shows that the fields gradually "pushed out" of the plasma region as the free-carrier density is increased. For the TE mode, this results in a gradual re-distribution of the field intensity, with the fields remaining continuous. The TM mode, by contrast, shows a marked redistribution of the fields. when the plasma has a sufficiently high density of carriers, the fields have gone from having a maximum in the center to the waveguide to having a maximum at the surface of the plasma. This substantial change in the fields is accompanied by a similar change in the propagation constant, resulting in a large phase shift. This relatively large mode shape change could possibly result in field reflections in the waveguide.

III. Plasma Distributions

The plasma generation due to an incident photon flux occurs in a region adjacent to the air/semiconductor interface. For photon energies of approximately $E_{ph} = 3.5$ eV, the absorption coefficients of GaAs and Si are about 10^6 cm^{-1}. Consequently, the e^{-1} absorption depth for the light is about 0.01 μm. If we consider using an injection laser source with $E_{ph} = 1.55$eV, the absorption coefficient in GaAs is only about 10^4 cm^{-1}. This corresponds to carrier generation occuring in a 1-μm layer near the surface.

In this section, we present a solution of the carrier diffusion equation in a semiconductor assuming the carriers are generated by an exponentially absorbed source. The carrier diffusion lengths are assumed to be much smaller than the waveguide width.

Diffusion

The analysis begins with the solution to the diffusion equation for excess carriers due to an incident laser beam of power P_0 watts/cm^2 at the surface $x=0$. In steady state, the excess carriers $N(x)$ satisfy

$$L_D^2\frac{d^2N}{dx^2}-N=-\tau R(x) \tag{5}$$

where L_D is the carrier diffusion length, τ is the spontaneous carrier lifetime, and R is the pump due to the incident laser beam. Since the light injected into the semiconductor waveguide is attenuated, the position-dependent pump rate $R(x)$ satisfies

$$R(x)=\frac{\eta\alpha_l}{h\nu}P_0e^{-\alpha_l x} \tag{6}$$

where η is the internal efficiency, α_l is the light absorption coefficient, $h\nu$ is the photon energy, and P_0 is the light power at $x=0$.

The solution of (5) with appropriate boundary conditions is

$$N(x)=\frac{\tau\eta\alpha_l P_0}{h\nu\left(\alpha_l^2L_D^2-1\right)}\left\{\frac{a_lL_D+S\tau/L_D}{1+S\tau/L_D}e^{-x/L_D}-e^{-\alpha_l x}\right\} \tag{7}$$

where S is the surface recombination velocity. $S\approx10^5$ cm/s for unpassivated Si and GaAs. However, with a properly prepared Si surface, S can be much smaller. If we assume $\alpha_lL_D\gg1$ and $\alpha_lL_D\gg S\tau/L_D$, then (7) can be approximated as

$$N(x)=N_0e^{-x/L_D} \tag{8}$$

where the carrier density at the surface is

$$N_0=\frac{\tau\eta P_0}{h\nu L_D(1+S\tau/L_D)}. \tag{9}$$

The excess carrier distribution given by (8) is identical to the one obtained by assuming the carriers are generated in a surface layer.

On the other hand, if the diffusion length L_D is small compared to the absorption depth $1/\alpha_l$, then the excess carrier distribution becomes

$$N(x)=N_0e^{-\alpha_l x} \tag{10}$$

where $N_0=\tau\eta\alpha_lP_0/h\nu$.

In both of the limiting cases discussed above, the carrier density has an exponential dependence. Therefore, we will study the effects of these distributions on the modal behavior in the simeconductor waveguides. The dielectric constant in the waveguide is given by (1). Since the dielectric constant is proportional to the square of the plasma frequency, the corresponding dielectric constant will be proportional to the carrier density.

IV. Electromagnetic Fields in Nonuniform Guide

When the dielectric constant is nonuniform due to the induced carrier profiles, it is difficult to find closed-form solutions to the field equations. However, in the special case of an exponential dielectric profile inside the semiconductor as obtained from (8), the wave can be solved in closed form [14]. To determine the eigenmodes, the fields must be matched at the two semiconductor/air interfaces. The resulting mode eigenvalues are determined from a rather complicated secular equation containing Bessel functions with complex arguments.

A more general approach is one where the complex wave equation is solved numerically using a multipoint boundary-value differential equation solver. The formulation of this problem is given in the Appendix. We have tested our results using various dielectric profiles. One example of the field solutions obtianed from COLSYS was for a dielectric slab waveguide with a uniform plasma layer as discussed earlier. Results were identical to those obtained from closed-form solutions.

The mathematical formulation of this problem is very different for the TE and TM modes. However, for both cases, the wave equation was reduced to two second-order (real and imaginary) differential equations. The COLSYS code is formulated such that solutions of simultaneous differential equations of arbitrary order are obtained. However, the continuity or "smoothness" of the solution is one degree less than the equation orders. For example, a differential equation of order n as given by $d^nf/dx^n=g(x)$ has solutions in $f\in C^{n-1}$ space. Thus, for $n=2$, the solutions have smooth first-order derivatives, but d^2y/dx^2 has discontinuities.

TE Modes

Because the wave equation can be separated into two second-order differential equations, the problem formulation is straightforward. The complex wave functions ψ are solutions of (A3) as given in the Appendix. Since the maximum order of the two simultaneous equations is 2, the wave functions have continuous first-order derivatives inside the semiconductor waveguide. The eigenvalues γ defining the propagation constants were obtained with relative errors less than 10^{-5}.

The propagation constants β and wave attenuation coefficients α obtained from solutions were used to calculate the relative phase shifts and attenuation of the modes over a 1-cm length of waveguide. The differential values were calculated from the α,β values in the passive waveguides and those obtained in the active one. In Figs. 6 and 7, we show the results obtained for Si and GaAs waveguides with exponential plasma profiles of the form $N_0\exp(-x/W_d)$ where N_0 is the plasma density at the surface. The abcissa is the value of N_0. The parameter W_d represents the diffusion length L_D in (8) when $\alpha_lL_D\gg1$, whereas w_d represents $1/\alpha_l$ in (10) when $\alpha_lL_D\ll1$.

The phase shift and attenuation performances are similar to those obtained using the uniform plasma layer model. However, we note that although the attenuation exhibits a resonance-type behavior, it does not go to zero at high plasma densities. This occurs because of the exponential tails of the carrier profiles which extend into the semiconductor material. In slab plasma layers, the fields are more easily pushed from the slab. In Figs. 8 and 9, the

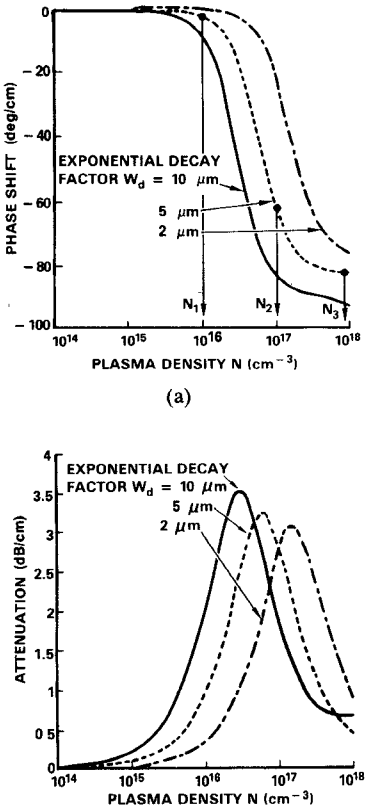

Fig. 6. The propagation characteristics for a TE mode in a silicon waveguide with an exponential plasma layer of various decay constants W_d. (a) The phase shift and (b) attenuation.

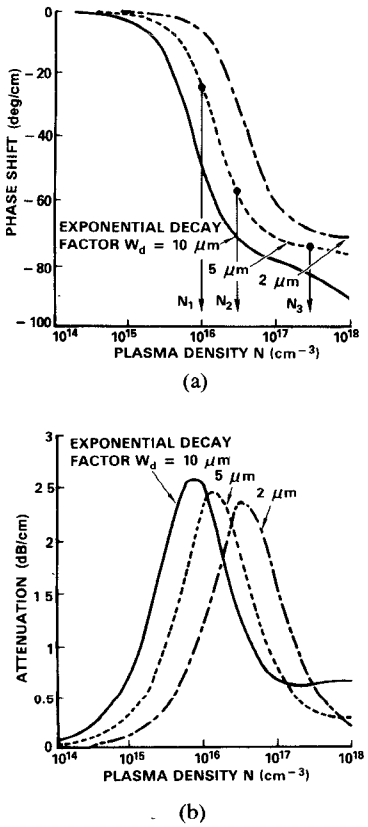

Fig. 7. The propagation characteristics for a TE mode in a gallium-arsenide waveguide with an exponential plasma layer of various decay constants w_d. (a) The phase shift and (b) attenuation.

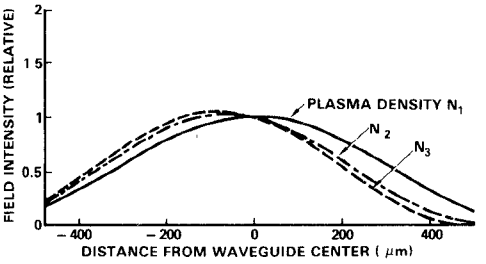

Fig. 8. The electric field intensity of the TE mode in a silicon nonuniform waveguide with a 5-μm exponential carrier decay. The different curves are for various plasma densities at the surface, located at 500 μm in the figure.

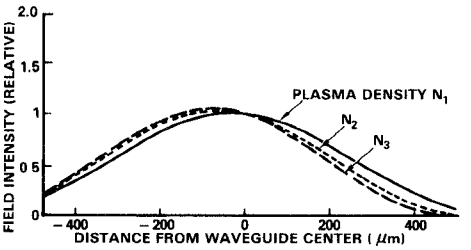

Fig. 9. The electric field intensity of the TE mode in a gallium arsenide nonuniform waveguide with a 5-μm exponential carrier decay. The different curves are for various plasma densities at the surface, located at 500 μm in the figure.

fields are plotted for $W_d = 5$ μm and various plasma densities at the surface. When $N_0 \approx 10^{16}\,\mathrm{cm}^{-3}$, the mode profiles are almost symmetrical, while for N_0 values $\approx 10^{18}$, the fields are being pushed toward the opposite side of the semiconductor slab.

TM Modes

In contrast to the TE mode, the field interaction of the TM mode with the plasma layer is pronounced. Relative phase shifts and attenuations are larger at the high plasma densities. In addition, the mathematical formulation is more complicated. In the Appendix, we have reduced the two second-order differential equations to a series of first-order ones. This was necessary because of the nature of the differential equation as given by (A10). The form of the equation is such that we must calculate the functional dependence $d\kappa/dx$ inside the waveguide. Although $d\kappa/dx$ is a well-behaved function for the exponential profiles, it has a discontinuity for the uniform plasma slabs. However, with proper formulation as that given in the Appendix, it is not necessary to compute the $d\kappa/dx$ functional dependence.

The phase shift and attenuation performance for the TM modes in Si and GaAs semiconductor waveguides are shown in Figs. 10 and 11 for the various exponential profiles. The major contrast between these solutions and those obtained using the slab plasma model is that attenuation does not significantly decrease for the case of high surface plasma densities using the nonuniform plasma model, especially for the thicker plasma regions.

The mode patterns of the TM waves are shown in Figs. 12 and 13. They were obtained for a 5-μm exponential carrier density with maximum values occuring at the surfaces. It should be noted that the high N_0 values

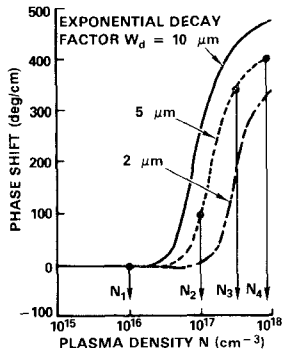

(a)

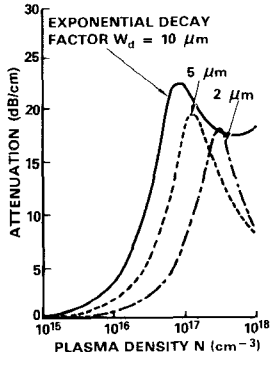

(b)

Fig. 10. The propagation characteristics for a TM mode in a silicon waveguide with an exponential plasma layer of various decay constants W_d. (a) The phase shift and (b) attenuation.

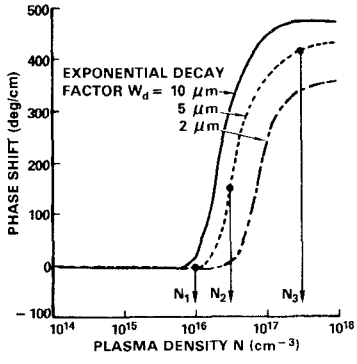

(a)

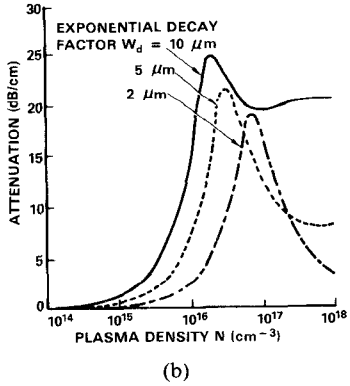

(b)

Fig. 11. The propagation characteristics for a TM mode in a gallium arsenide waveguide with an exponential plasma layer of various decay constants W_d. (a) The phase shift and (b) attenuation.

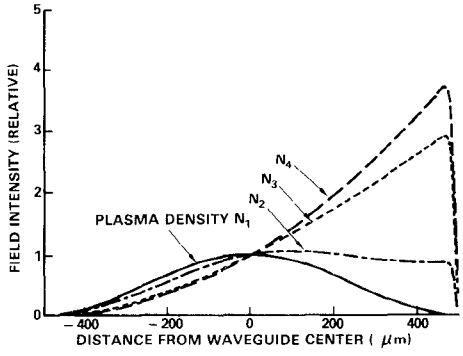

Fig. 12. The electric field intensity of the TM mode in a silicon nonuniform waveguide with a 5-μm exponential carrier decay. The different curves are for various plasma densities at the surface, located at 500 μm in the figure.

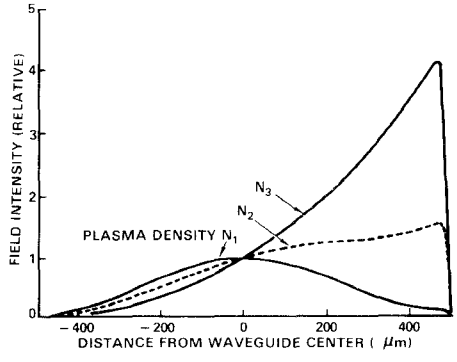

Fig. 13. The electric field intensity of the TM mode in a gallium arsenide nonuniform waveguide with a 5-μm exponential carrier decay The different curves are for various plasma densities at the surface, located at 500 μm in the figure.

produce a plasma surface wave since the field energy is concentrated near the surface.

V. Conclusion

An analysis of the millimeter-wave phase shifter has been presented. The phase shift is obtained by altering the dielectric constant of a semiconductor waveguide by photo-excitation of electron/hole pairs. Our analysis treats a nonuniform carrier distribution in the waveguide, in contrast to earlier treatments using a uniform layer model. The nonuniform plasma model has been applied to an exponentially absorbed optical beam. The model reveals that wave attenuation does not approach zero as the plasma density increases, in contrast to the uniform layer model results. The behavior of the phase shift as a function of plasma density is similar for both models.

The field distributions in the phase shifter have also been plotted for both the uniform and nonuniform layer models. The field distributions show that the high phase shift of the TM mode is accomplished by a strong distortion of the field from that in the passive dielectric waveguide. On the other hand, the fields of the TE mode change very little from that obtained in the passive waveguide to those of the active structure.

The model reported here is of a general nature and can be used to analyze a variety of spatial profiles of the complex dielectric constant in waveguides. We are pre-

sently using the model to analyze nonuniform guides at optical frequencies.

APPENDIX

We have solved Maxwell's equations by numerical techniques using software developed for multiple-point boundary-value problems. The dielectric waveguide of Fig. 1 can be approximated using a multiple-layer waveguide where the dielectric constant is layer dependent. However, in the case where the electron/hole pairs are generated at the surface of the dielectric waveguide, the carriers diffuse to interior points. The resulting pair density will have a exponential behavior along x so that the complex dielectric constant $\kappa(x) = \kappa_0 e^{-x/x_0}$. Since the dielectric constant varies continuously along x, we use numerical techniques to solve the wave equation. We assume the modes propagate along z according to $e^{j\omega t - \gamma z}$ where $\gamma = \alpha + j\beta$ is the complex propagation constant.

TE Mode

In the slab waveguide model, the field components are independent of y. For the TE wave, we assume the component $E_y = \psi(x)e^{j\omega t - \gamma z}$. The remaining fields are

$$H_x = \frac{\gamma}{j\omega\mu} E_y \tag{A1}$$

$$H_z = -\frac{1}{j\omega\mu}\frac{\partial E_y}{\partial x}. \tag{A2}$$

The wave function ψ satisfies the wave equation

$$\frac{d^2\psi}{dx^2} + \left[\gamma^2 + k_0^2\kappa(x)\right]\psi = 0 \tag{A3}$$

where $\kappa(x)$ defines the relative dielectric constant.

Since the wave function $\psi = \psi_r + j\psi_i$ is complex, the above equation becomes

$$\frac{d^2\psi_r}{dx^2} = -\left[(\alpha^2 - \beta^2) + k_0^2(n^2 - k^2)\right]\psi_r + 2\left[\alpha\beta - k_0^2 nk\right]\psi_i \tag{A4a}$$

$$\frac{d^2\psi_i}{dx^2} = -2\left[\alpha\beta - k_0^2 nk\right]\psi_r - \left[(\alpha^2 - \beta^2) + k_0^2(n^2 - k^2)\right]\psi_i \tag{A4b}$$

where we have $\kappa = (n - jk)^2$, n is the refractive index and k is the extinction coefficient.

Since the computational package COLSYS solves a multipoint boundary problem, we add two extra differential equations

$$\frac{d\alpha}{dx} = 0 \tag{A5a}$$

$$\frac{d\beta}{dx} = 0 \tag{A5b}$$

which allows for the computation of the complex eigenvalues γ.

Outside the dielectric waveguide, the field solutions can be written in terms of wavefunction and eigenvalues at $x = d_u$, the upper boundary, and $x = d_l$, the lower boundary. In regions 1 and 3, the air field solutions are

$$\psi_1 = \psi(d_u)e^{p(d_u - x)} \tag{A6a}$$

$$\psi_3 = \psi(d_l)e^{p(-d_l + x)} \tag{A6b}$$

where $p^2 = -(\gamma^2 + k_0^2)$. The total number of boundary equations (4) at the two interfaces is obtained by matching the magnetic fields

$$\frac{d\psi(d_u)}{dx} + p\psi(d_u) = 0 \tag{A7a}$$

$$\frac{d\psi(d_l)}{dx} - p\psi(d_l) = 0. \tag{A7b}$$

Since the total order of the system of equations is six, we arbitrarily set the field at $x = 0$ (center point of guide) to $\psi(0) = 1$ giving us a total of six boundary equations. This last boundary condition sets the field magnitude to unity with a zero phase shift.

TM Mode

The TM modes have the field components E_x, E_z, and H_y. Here, we set $H_y = \phi(x)e^{j\omega t - \gamma z}$ and the remaining field components become

$$E_x = \frac{\gamma}{j\omega e_0\kappa(x)} H_y \tag{A8}$$

$$E_z = \frac{1}{j\omega e_0\kappa(x)}\frac{\partial H_y}{\partial x}. \tag{A9}$$

The wave function ϕ satisfies

$$\kappa(x)\frac{\partial}{\partial x}\left[\frac{1}{\kappa(x)}\frac{\partial\phi}{\partial x}\right] + \left[\gamma^2 + k_0^2\kappa(x)\right]\phi = 0 \tag{A10}$$

while the eigenvalue satisfies $\partial\gamma/\partial x = 0$.

The solution of (A10) is more complicated to obtain from COLSYS than for (A3) because the derivative of the dielectric constant appears in the differential equation. Consequently, it is convenient to reduce (A10) to a series of first-order equations of the real variables

$$\Phi_1 = \alpha \tag{A11a}$$

$$\Phi_2 = \beta \tag{A11b}$$

$$\Phi_3 = \phi_r \tag{A11c}$$

$$\Phi_4 = \frac{1}{|\kappa|^2}\left[\kappa_r\frac{d\phi_r}{dx} + \kappa_i\frac{d\phi_i}{dx}\right] \tag{A11d}$$

$$\Phi_5 = \phi_i \tag{A11e}$$

$$\Phi_6 = \frac{1}{|\kappa|^2}\left[\kappa_r\frac{d\phi_i}{dx} - \kappa_i\frac{d\phi_r}{dx}\right]. \tag{A11f}$$

The resulting set of differential equations become

$$\frac{d\Phi_1}{dx} = 0 \tag{A12a}$$

$$\frac{d\Phi_2}{dx} = 0 \tag{A12b}$$

$$\frac{d\Phi_3}{dx} = \kappa_r\Phi_4 - \kappa_i\Phi_6 \tag{A12c}$$

$$\frac{d\Phi_4}{dx} = \frac{1}{|\kappa|^2}\left\{-\left(\Phi_1^2 - \Phi_2^2 + \kappa_r\right)\left(\kappa_r\Phi_3 + \kappa_i\Phi_5\right) + \left(2\Phi_1\Phi_2 + \kappa_i\right)\left(\kappa_r\Phi_5 - \kappa_i\Phi_3\right)\right\} \tag{A12d}$$

$$\frac{d\Phi_5}{dx} = \kappa_i\Phi_4 + \kappa_r\Phi_6 \tag{A12e}$$

$$\frac{d\Phi_6}{dx} = \frac{1}{|\kappa|^2}\left\{-\left(\Phi_1^2 - \Phi_2^2 + \kappa_r\right)\left(\kappa_r\Phi_5 - \kappa_i\Phi_3\right) - \left(2\Phi_1\Phi_2 + \kappa_i\right)\left(\kappa_r\Phi_3 + \kappa_i\Phi_5\right)\right\}. \tag{A12f}$$

The field solutions outside the semiconductor are

$$\phi_1 = \phi(d_u)\, e^{p(d_u - x)} \tag{A13a}$$

$$\phi_3 = \phi(d_l)\, e^{p(-d_l + x)} \tag{A13b}$$

where $p^2 = -(\gamma^2 + k_0^2)$. In terms of the variables Φ_i, the eigenvalues $\gamma = \Phi_1 + j\Phi_2$.

The boundary conditions used in COLSYS are

$$\kappa_r\Phi_4(d_l) - \kappa_i\Phi_6(d_l) - \left[\kappa_r p_r - \kappa_i p_i\right]\Phi_3(d_l) + \left(\kappa_i p_r + \kappa_i p_r\right)\Phi_5(d_l) = 0 \tag{A14a}$$

$$\kappa_i\Phi_4(d_l) + \kappa_r\Phi_6(d_l) - \left[\kappa_i p_r + \kappa_r p_i\right]\Phi_3(d_l) - \left(\kappa_r p_r - \kappa_i p_i\right)\Phi_5(d_l) = 0 \tag{A14b}$$

$$\Phi_3(d_0) - 1 = 0 \tag{A14c}$$

$$\Phi_5(d_0) = 0 \tag{A14d}$$

$$\kappa_r\Phi_4(d_u) - \kappa_i\Phi_6(d_u) + \left(\kappa_r p_r - \kappa_i p_i\right)\Phi_3(d_u) - \left(\kappa_i p_r + \kappa_r p_i\right)\Phi_5(d_u) = 0 \tag{A14e}$$

$$\kappa_i\Phi_4(d_u) + \kappa_r\Phi_6(d_u) + \left(\kappa_i p_r + \kappa_r p_i\right)\Phi_3(d_u) + \left(\kappa_r p_r - \kappa_i p_i\right)\Phi_5(d_u) = 0. \tag{A14f}$$

The boundary conditions in (A14a) and (A14b) are obtained by matching the axial component of the electric field E_z at $x = d_1$. Equations (A14e) and (A14f) are obtained from matching E_z at $x = d_u$. The remaining two boundary conditions are obtained by arbitrarily setting the wave function $\phi = 1$ at $x = d_0$.

References

[1] F. Stern, "Optical properties of semiconductors," in *Solid State Physics, Advances and Applications*, H. Ehrenrich, F. Seitz, and D. Turnbull, Eds. New York: Academic Press, 1963.

[2] H. Jacobs and M. M. Chrepta, "Electronic phase shifter for millimeter wave semiconductor dielectric integrated circuits," *IEEE Trans. Microwave Theory Tech.*, vol. MTT-22, pp. 411–417, Apr. 1974.

[3] B. J. Levin and G. G. Weidner, "Millimeter-wave phase shifter," *RCA Rev.*, vol. 34, pp. 489–505, 1973.

[4] B. Glance, "A fast low loss microstrip p-i-n phase shifter," *IEEE Trans. Microwave Theory Tech.*, vol. MTT-27, pp. 14–16, Jan. 1979.

[5] B. J. Levin and G. Weidner, "A distributed pin diode phaser for millimeter wavelengths," in *IEEE MTT-S Int. Symp. Dig.*, 1973, pp. 63–65.

[6] G. R. Vanier and R. M. Mindock, "Diode structures for a millimeter wave shifter," in *IEEE MTT-S Int. Symp. Dig.*, 1975, pp. 173–175.

[7] C. H. Lee, P. S. Mak, and A. P. DeFonzo, "Optical control of millimeter-wave propagation in dielectric waveguides," *IEEE J. Quantum Electron.*, vol. QE-16, pp. 277–288, Mar. 1980.

[8] A. M. Vaucher, C. D. Striffler, and C. H. Lee, "Theory of optically controlled millimeter-wave phase shifters," *IEEE Trans. Microwave Theory Tech.*, vol. MTT-31, pp. 209–216, Feb. 1983.

[9] I. Gladwell, "Shooting codes in the NAG library," in *Lecture Notes in Computer Science*, vol. 76, B. Childs *et al.*, Eds. New York: Springer-Verlag, 1979.

[10] V. Asder, J. Christiansen, and R. D. Russel, "COLSYS—A collocation code for boundary value problems," *Lecture Notes in Computer Science*, vol. 76, B. Childs *et al.*, Eds. New York: Springer-Verlag, 1979.

[11] E. A. J. Marcatili, "Dielectric rectangular waveguide and directional couplers for integrated optics," *Bell Syst. Tech. J.*, vol. 48, pp. 2071–2102, Sept. 1969.

[12] M. N. Afsar and K. J. Button, "Precise millimeter-wave measurements of complex refractive index, complex dielectric permittivity and loss tangent of GaAs, Si SiO_2, Al_2O_3, BeO, macor, and glass," *IEEE Trans. Microwave Theory Tech.*, vol. MTT-31, pp. 217–223, Feb. 1983.

[13] S. M. Sze, *Physics of Semiconductor Devices*, 2nd ed. New York: Wiley, 1981.

[14] I. P. Kaminow, W. L. Mammel, and H. P. Weber, "Metal-clad optical waveguides: Analytical and experimental study," *Appl. Opt.*, vol. 13, pp. 396–405, 1974.

✠

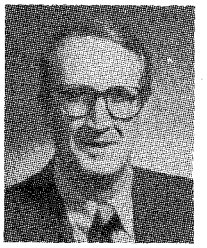

Jerome K. Butler (S'59–M'65–SM'78) was born in Shreveport, LA, on September 27, 1938. He received the B. S. degree from Louisiana Polytechnic Institute, Ruston, in 1960, and the M. S. and Ph. D. degrees from the University of Kansas, Lawrence, in 1962 and 1965, respectively.

From 1960 to 1965, he was a Research Assistant at the Center for Research in Engineering Sciences, University of Kansas. His research was related to electromagnetic-wave propagation and to the optimization and synthesis techniques of antenna arrays. In 1965, he joined the staff of the School of Engineering and Applied Science, Southern Methodist University, Dallas, TX, where he is now Professor of Electrical Engineering. His primary research areas are solid-state injection lasers, radiation and detection studies of lasers, communication and imaging systems, integrated optics and the application of integrated optical circuits, and quantum electronics. Every summer since 1969, he has served as a Member of the Technical Staff, RCA Laboratories, Princeton, NJ, where he conducts research concerned with electromagnetic-wave propagation in solid-state injection lasers. Dr. Butler is coauthor of the book *Semiconductor Lasers and Heterojunction LED's* published by Academic Press. He has held consulting appointments with the Central Research Laboratory of Texas Instruments, Inc., the Geotechnical Corporation of Teledyne, Inc., Earl Cullum Associates of Dallas, TX, and the University of California Los Alamos Scientific Laboratory.

Dr. Butler is a member of Sigma Xi, Tau Beta Pi, Eta Kappa Nu, and is a registered professional engineer in the state of Texas.

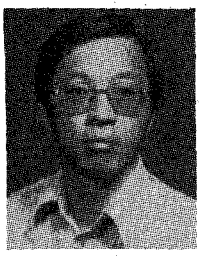

Tran-Fu Wu was born in Naking, Republic of China, on October 24, 1947. He received the B. S. degree in electrical engineering from the Chung Cheng Institute of Technology, Taipei, Taiwan, in 1970 and the M.S.E.E. degree from Northwestern University, Evanston, IL, in 1978. He is currently working toward a Ph.D. degree.

His research interests are bulk GaAs lasers and plasma millimeter-wave interaction in dielectric waveguides.

Marion Scott (S'73–M'78) was born in Oklahoma City, OK, on February 21, 1952. He received the B. S., M. S., and Ph.d degrees in electrical engineering from Southern Methodist University in 1975, 1976, and 1979, respectively.

His research in graduate school was in the area of dielectric optical waveguides for integrated optics applications. He joined LTV Aerospace and Defense in 1979, where he has participated in the design, analysis, construction, and testing of 10.6-μm scan lasers. He has also worked on agile sensors and other devices using vanadium dioxide technology. He is presently engaged in developing new components for the millimeter-wave regime.

Dr. Scott is a member of the Optical Society of America, Sigma Xi, and Tau Beta Pi.